

An improved lower bound for superluminal quantum communications.

Bruno Coccia,^{*} Sandro Faetti,[†] and Leone Fronzoni[‡]
Department of Physics Enrico Fermi, Largo Pontecorvo 3, I-56127 Pisa, Italy.
(Dated: May 29, 2022)

Superluminal communications have been proposed to solve the Einstein, Podolsky and Rosen (*EPR*) paradox. So far, no evidence for these superluminal communications has been obtained and only lower bounds for the superluminal velocities have been established. In this paper we describe an improved experiment that increases by about two orders of magnitude the maximum detectable superluminal velocities. The locality, the freedom-of-choice and the detection loopholes are not addressed here. No evidence for superluminal communications has been found and a new higher lower bound for their velocities has been established.

PACS numbers: 03.65.Ud, 03.67.Mn

In 1935 Einstein, Podolsky and Rosen [1] showed that the orthodox Quantum Mechanics (*QM*) is a non-local theory (*EPR* paradox). Consider, for instance, the two photons *a* and *b* in Figure 1 that propagate in opposite directions and that are in the polarization entangled state

$$|\psi\rangle = \frac{1}{\sqrt{2}} (|H, H\rangle + |V, V\rangle) \quad , \quad (1)$$

where *H* and *V* denote horizontal and vertical polarization, respectively. According to *QM*, a polarization measurement on photon *a* leads to the instantaneous collapse of the polarization state of photon *b* whatever is its distance from *a*. This behavior is reminiscent of the action at a distance that has been completely rejected by the modern General Relativity and Electromagnetism theories. For this reason, Einstein et al. believed that *QM* is a not complete theory and suggested that a complete theory should contain some additive local variables. In 1961 J. Bell showed [2] that any theory based on local variables must satisfy an inequality that is violated by *QM*.

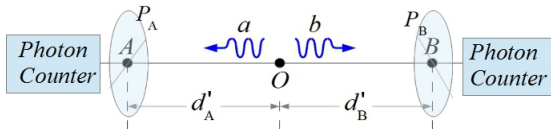


Figure 1. Two entangled photons *a* and *b* are generated at *O* and get polarizers *P*_{*A*} (Alice polarizer) and *P*_{*B*} (Bob polarizer).

Analogous inequalities have been found by Clauser et al. [3, 4]. The Aspect experiment of 1982 [5] demonstrated that the Bell inequality is not satisfied and also showed that quantum correlations cannot be established by subluminal or luminal communications. Then, some physicists suggested [6, 7] that the correlations between entangled particles could be due to superluminal communications [8] (*v*-causal models in nowadays literature [9]). To avoid causal paradoxes, they assumed that a preferred frame (*PF*) exists where superluminal signals propagate isotropically with unknown velocity $v_t = \beta_t c$.

It has been shown [10, 11] that *v*-causal models leads to superluminal communications in the macroscopic world (signalling). Although one of us believes that signalling is not incompatible with the Relativity theory [12, 13], most physicists think that there is no compatibility and, thus, the experimental evidence of signalling should need a revision of the Relativity theory. In standard conditions, the superluminal communications lead to the *QM* correlations but there are special conditions (if the second particle reaches its measurement device when the collapsing wave didn't reaches it) where the *QM* correlations cannot be established and the Bell inequality must be satisfied. In fact, if polarizers *P*_{*A*} and *P*_{*B*} in Figure 1 are at the same optical distances *d'*_{*A*} and *d'*_{*B*} from source *O* in the *PF*, the two photons get them simultaneously and, thus, there is no time to establish *QM* correlations. To verify this behavior, one can measure the correlation parameter *S*_{*max*} defined as [14, 15]

$$S_{\max} = P_0 - \sum_{i=1}^3 P_i \quad , \quad (2)$$

with $P_0 = P(45^\circ, 67.5^\circ)$, $P_1 = P(0^\circ, 67.5^\circ)$, $P_2 = P(45^\circ, 112.5^\circ)$ and $P_3 = P(90^\circ, 22.5^\circ)$, where $P(\alpha, \xi)$ is the probability that photon *a* passes through polarizer *P*_{*A*} aligned at the angle α with respect to the horizontal plane and that photon *b* passes through polarizer *P*_{*B*} aligned at the angle ξ . *S*_{*max*} must satisfy the inequality [14, 15] $S_{\max} \leq 0$ whilst *QM* predicts $S_{\max} = (\sqrt{2}-1)/2 \approx 0.2071$. Probabilities $P(\alpha, \xi)$ are given by

$$P(\alpha, \xi) = \frac{N(\alpha, \xi)}{N_{\text{tot}}} \quad , \quad (3)$$

where $N(\alpha, \xi)$ are the coincidences between entangled photons passing through the polarizers during the acquisition time Δt and N_{tot} is the total number of entangled photons couples that can be obtained using eq.(4)[15]:

$$N_{tot} = \sum_{i=0}^3 N_i, \quad (4)$$

where $N_0 = N(0^\circ, 0^\circ)$, $N_1 = N(0^\circ, 90^\circ)$, $N_2 = N(90^\circ, 0^\circ)$ and $N_3 = N(90^\circ, 90^\circ)$. If $d'_A = d'_B$, the quantum correlations cannot be established and S_{max} should always satisfy the inequality [14, 15] $S_{max} \leq 0$. Due to the experimental uncertainty Δd on the equalization of the optical paths in the *PF*, the entangled photons may not get the polarizers simultaneously and a communication can yet occur if velocity β_t of the superluminal signals is greater than the maximum detectable value $\beta_{t,max} = d'_{AB}/\Delta d$, where d'_{AB} is the distance from *A* to *B* in the *PF* (see Figure 1). In the Earth frame, the equalization of distances d_A and d_B does not implies their equalization also in the *PF* except if the unknown velocity vector $\vec{V} = \vec{\beta} c$ of the *PF* with respect to the Earth frame satisfies the orthogonality condition $\vec{\beta} \cdot \vec{AB} = 0$. Due to the Earth rotation around its axis, if the *AB* segment is East-West aligned, there are always two times t_1 and t_2 for each sidereal day where \vec{AB} becomes orthogonal to $\vec{\beta}$ [16, 17]. At these times, S_{max} should exhibit a breakdown from the quantum value $S_{max} = 0.207$ toward $S_{max} \leq 0$. In terms of the Earth experimental parameters, the maximum detectable velocity $\beta_{t,max}$ becomes [16, 17]

$$\beta_{t,max} = \sqrt{1 + \frac{(1 - \beta^2)[1 - \rho^2]}{[\rho + \beta \sin \chi \sin \frac{\pi \delta t}{T}]^2}}, \quad (5)$$

where χ is the unknown angle that the velocity of the *PF* makes with the Earth rotation axis, T is Earth rotation day, $\rho = d_{AB}/\Delta d$ and δt is the measurement time of S_{max} , where d_{AB} is the distance between points *A* and *B* in the Earth Frame and Δd is the uncertainty in the equalization of the optical paths. Experimental tests of the superluminal models have been reported in the literature but, so far, no evidence for a violation of *QM* predictions has been found and only lower bounds $\beta_{t,max}$ have been obtained [15–18]. In reference [18], the locality and freedom-of-choice loopholes were also addressed. Here we report the results of a new experiment where the loopholes above are not taken into account but the maximum detectable velocities of the superluminal communications are increased by about two orders of magnitude. In particular, according to [19] we here test the “assumption that quantum correlations are due to supra-luminal influences of a first event onto a second event”. Since we use absorption polarizing films, we assume that the above events are the collapses of the polarization state that occur when the photons hit the polarizers.

Our experimental apparatus, the procedures used to obtain very small values of the basic experimental parameters ρ and δt and the experimental uncertainties

have been described in detail in a previous paper [15] and, thus, we will remind here only the main features. To get a small value of $\rho = d_{AB}/\Delta d$ we perform our measurements in the so called "East-West" gallery of the European Gravitational Observatory (*EGO*) of Cascina and we use an interferometric method to equalize the optical paths d_A and d_B ($d_A \approx d_B \approx 600$ m). Unfortunately, the *EGO* gallery makes the angle $\gamma = 18^\circ$ with the East-West axis and the orthogonality condition $\vec{\beta} \cdot \vec{AB} = 0$ is never satisfied if the velocity vector of the *PF* makes an angle $\chi < \gamma = 18^\circ$ with respect to the Earth rotation axis. Then, our experiment is insensitive to $\approx 5\%$ of all the possible alignments of the *PF* velocity vector. Note that the Reference Frame of the Cosmic Microwave Background (*CMB*) is accessible to our experiment. A pump laser beam at a wavelength 406.3 nm generated by a 220 mW laser diode passes through a Glan-Thompson polarizer, a motorized $\lambda/2$ plate, a motorized Babinet-Soleil compensator and is focused (spot diameter = 0.6 mm) by an achromatic lens at the center of two thin (thickness 0.5 mm) adjacent *BBO* nonlinear optical crystals plates cut for *type I phase matching* [20]. Down conversion leads to two outgoing beams of entangled photons at the average wavelength $\lambda = 812.6$ nm that mainly propagate at two symmetric angles ($\pm 2.4^\circ$) with respect to the normal to the *BBO* plates. Using the compensation procedures developed by the Kwiat group [21–23], we get a high intensity source of entangled photons ($N \approx 23000$ counts/s). A proper system of mirrors deviates the two entangled beams in two opposite directions along the *EGO* gallery. The entangled beams are collected by large diameter (15 cm) achromatic lenses having a long focal length (6.00 m). The beams outgoing from the lenses impinge on two identical lenses at a distance of 600 m and produce two 1:1 images (0.6 mm-width) of the source of the entangled photons at the centers of the Thorlabs *LPVIS* linear polarizers layers P_A and P_B . Four reference beams at wavelength 681 nm are generated by a superluminous diode and are used to align the optical system, to equalize the optical paths and to build a feedback to stabilize the images of the source at the center of the two polarizers within ± 0.5 mm [15]. Each of the entangled photons beams outgoing from the two polarizers passes through two long-pass optical filters and a band-pass filter (40 nm-width) centered at the wavelength $\lambda = 810$ nm and is focused on a $200 \mu\text{m}$ multimode optical fiber connected to a Perkin Elmer photons counter module. The output pulses of the photons counters are transformed into optical pulses (LCM155EW4932-64 modules of Nortel Networks) that propagate in two monomode optical fibers toward the temperature stabilized central optical table (within $\pm 0.1^\circ\text{C}$) where the entangled photons are generated. Finally, the optical pulses are transformed again into electric pulses and sent to an electronic coincidence circuit. An electronic counter counts the Alice pulses N_A , the Bob pulses N_B and the coincidences

pulses N . A Real Time Labview program running on a National Instruments CompactDAQ provides an accurate real time acquisition of coincidences and counts. To greatly reduce the S_{max} measurement time δt with respect to our previous experiment [15], we measure each of the four contributions appearing in eq.(2) in successive daily experimental runs. This procedure allows us to set the polarization angles α and ξ only one time each day to avoid the retardation due to the polarizers rotation [15]. We get $\rho = 1.83 \times 10^{-7}$ [15] and $\delta t = 0.494$ s that provide a $\beta_{t,max}$ value about two orders of magnitude higher than the previously measured values. All the measurements are automated using a Real Time Labview program. A *GPS* server provides the actual *UTC* time [24] with an accuracy better than 1 ms. Since the investigated phenomenon is strictly related to the Earth rotation, we synchronize the acquisitions with the Earth rotation time t that is related to the Earth Rotation Angle θ (*ERA* [24]) by the relation $t = \theta \times 240$ s where θ is expressed in degrees. The *ERA* time is related to the Julian day [24] by the simple linear relation: $t = 86400 \times (TJ \bmod 1)$ where “mod” represents the modulo operation and $TJ = [a_1 + b_1 \times (\text{Julian day} - 2451545.0)]$ with $a_1 = 0.7790572732640$ and $b_1 = 1.00273781191135448$. The IERS Bulletin A [25] provides the value of the daily difference $\Delta = UT1 - UTC$ between the *UT1* [24] time and the *UTC* time and, thus, *UT1* and the actual value of t can be obtained. The successive steps of the fully automated procedure are: 1- The Labview program reads the *GPS* Greenwich *UTC* time and the *IERS* *UTC-UT1* value, then, the Greenwich *ERA* time t is calculated. Finally, the *UTC* time that corresponds to the next zero value of the Greenwich *ERA* time is calculated. 2- Two hours before $t = 0$, the program rotates the P_A and P_B polarizers and sets successively the α and ξ angles that enter in N_{tot} in eq.(4). For each setting of the polarizers angles, the coincidences are measured for a 100 s time. The spurious coincidences $N_S = N_A \times N_B \times T_p$ are subtracted, where T_p is the pulses duration time. Finally, the total number of entangled photons N_{tot} in eq.(4) is calculated. 3- At the end of these preliminary measurements, the polarizer angles are set at $\alpha = 45^\circ$ and $\xi = 67.5^\circ$ appearing in the first contribution P_0 in eq.(2). Then, the program starts the acquisition of the coincidences when the Greenwich *ERA* time is 0 within ± 1 ms. The duration of a complete acquisition run is $T_0 = 36$ *ERA* hours with 10^{19} successive acquisitions that correspond to the acquisition time $\Delta t = T_0/10^{19} = 246.5174617015710825$ ms. To ensure a sufficient time precision we use the microseconds internal counter of the Real Time Labview and we correct each $10 \mu\text{s}$ for the errors due to the microseconds quantization of the counter. 4- At the end of the first acquisition run, the program calculates the 10^{19} values of P_0 and sets the second couple of angles α and ξ of the P_1 term in eq.(2). Then, procedure 1-4 is repeated until all probabilities P_i are obtained.

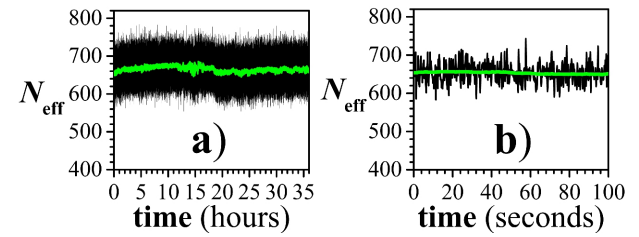


Figure 2. a) Effective coincidences (true + spurious) versus the Greenwich *ERA* time. The 10^{19} points are connected by black lines leading to the resulting black region in the Figure. The green full line is the result of smoothing averaging over 200 points. b) A detail of the coincidences during 100 s is shown.

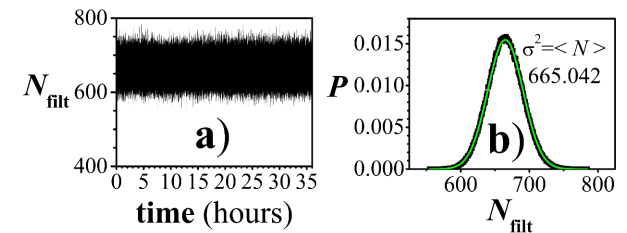


Figure 3. a) Filtered coincidences where the slow instrumental drift of the average value in Figure 2 has been subtracted. b) probability distribution of the coincidences (black points). The full green curve is the normal distribution predicted by the statistic theory of counts having $\sigma^2 = < N_{filt} > = 665.042$.

Figure 2(a) shows an example of effective coincidences (true+spurious) N_{eff} versus the Greenwich *ERA* time during a single run. The greater contribution to noise in our experiment is the statistical counts noise. This is evident if we eliminate the slow drift contribution and we plot the “filtered” coincidences $N_{filt} = N_{eff} - N(\text{smoothing}) + < N_{eff} >$. Figure 3(a) shows N_{filt} versus the *ERA* time whilst Figure 3(b) shows the correspondent probability distribution P (black points). The full green line in Figure 3(b) is not a best fit but is the Normal Gaussian function with fixed parameters $\sigma^2 = < N > = 665.042$ that is predicted by the Statistics of counts. Figures 4(a)-4(d) show the probabilities $P_i = P(\alpha_i, \xi_i) = N(\alpha_i, \xi_i)/N_{tot}$ obtained in the successive runs. The black region represents the measured values, the full green line represents the average value whilst the green dotted line represents the value predicted by *QM* for a pure entangled state (fidelity $F = 1$). The discrepancy between the full and dotted lines indicates that our entangled state is not completely pure ($F < 1$). In the simplest assumption that the breakdown of quantum correlations occurs with the Earth rotation periodicity one could calculate a S_{max} value by substituting the P_i contributions of Figures 4 measured at the same *ERA* time t in successive runs into the theoretical expression of S_{max} .

With this procedure we get the results shown in

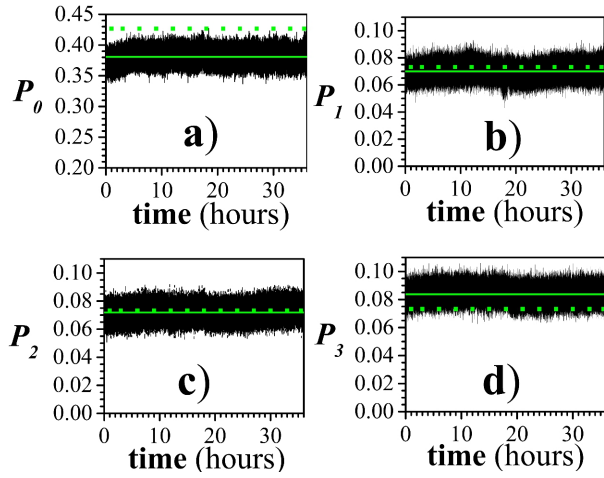


Figure 4. The black regions represents the measured probabilities P_0 , P_1 , P_2 and P_3 versus the Greenwich ERA time in successive experimental runs. 10^{19} probability values are shown that correspond to the acquisition time $\Delta t = 0.246$ s. The green full lines represent the average values of the measured probabilities: $\langle P_0 \rangle = 0.38087$, $\langle P_1 \rangle = 0.06999$, $\langle P_2 \rangle = 0.07187$, $\langle P_3 \rangle = 0.08378$. The green dotted lines correspond to the values predicted by QM for a pure entangled state: $P_0 = 0.4267$, $P_1 = P_2 = P_3 = 0.0732$.

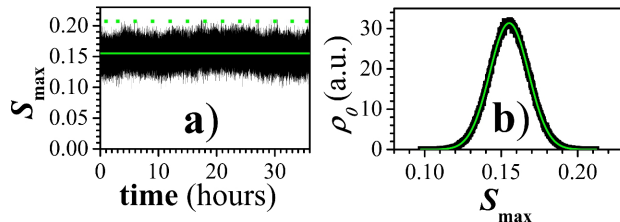


Figure 5. a) S_{max} versus the ERA time obtained using the relation $S_{max}(t) = P_0(t) - P_1(t) - P_2(t) - P_3(t)$. The green full line is the average value of $S_{max} = 1.5523$, whilst the green dotted line represents the QM value $S_{max} \approx 0.207$ for a pure entangled state. b) The Frequency Distribution ρ_0 of the 10^{19} measured values of S_{max} in arbitrary units is shown. The full green curve is the Gaussian fit with standard deviation $\sigma = 0.01272$ and $\langle S_{max} \rangle = 0.15523$.

Figure 5(a) (black region) and the corresponding Frequency Distribution ρ_0 shown in Figure 5(b) where black points represent the experimental results whilst the full green line is the best fit with the Gaussian function $A \exp \left[-\left(S_{max} - \langle S_{max} \rangle \right)^2 / (2\sigma^2) \right]$ with standard deviation $\sigma = 0.01272$ and $\langle S_{max} \rangle = 0.15523$. The green full line in Figure 5(a) shows the average value $\langle S_{max} \rangle$ whilst the green dotted line is the QM value $S_{max} = 0.2071$ for the pure entangled state in eq.(1)($F = 1$). The lower average value $\langle S_{max} \rangle$ seems to indicate that the fidelity of our state is appreciably lower than $F = 1$. No breakdown of S_{max} to zero is visible in Figure 5(a) but the analysis above is not sufficient to conclude that no

superluminal effect is present. In fact, the breakdown of the QM correlations is predicted to occur at the two times where $\vec{\beta} \cdot \vec{AB} = 0$. Due to revolution motion of the Earth around the sun and other motions (precession and nutation of the Earth axis), the orthogonality condition is not satisfied exactly at the same ERA times in different ERA days. Denote by t_{i1} and t_{i2} the two unknown orthogonality times during the i -th measurement run ($i = 0 - 3$) and by $P_i(t_{ij})$ with $i = 0 - 3$ and $j = 1, 2$ the corresponding probabilities measured at these times. These probabilities should be different from the QM values and the parameters

$$S_{max}(j) = P_0(t_{0j}) - \sum_{i=1}^3 P_i(t_{ij}), \quad (6)$$

with $j = 1, 2$, should be lower than zero if $\beta_t < \beta_{t,max}$.

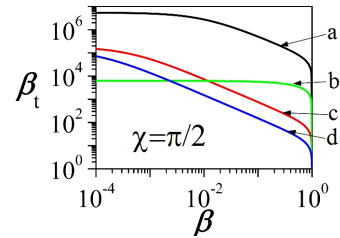


Figure 6. Curve *a* shows the $\beta_{t,max}$ values obtained in our experiment versus the unknown velocity β of the PF for the unfavorable case $\chi = \pi/2$; curve *b* is the result given in reference [17]; curve *c* that given in reference [16] and curve *d* that given in reference [18]. Note that only in the case of curve *d* the locality and freedom-of-choice loopholes were addressed.

We do not know times t_{ij} but it is obvious that $S_{max}(j) \geq S = \text{MIN}(P_0) - \text{MAX}(P_1) - \text{MAX}(P_2) - \text{MAX}(P_3)$ where $\text{MIN}(P_i)$ and $\text{MAX}(P_i)$ denote the absolute minimum and maximum values of P_i , respectively. From the data in Figures 4 we get $S = 0.04237$ and, thus $S_{max}(j) \geq 0.04237 \approx 3.3 \sigma$. The probability that a value of $S_{max}(j)$ lower or equal to zero could be compatible with our measured values is $p \leq \frac{1}{2} \text{erfc} \left[0.04237 / (\sqrt{2}\sigma) \right] = 4.3 \cdot 10^{-4}$ where $\text{erfc}(x)$ is the complementary error function. Thus, the probability that two breakdowns ($j = 1$ and $j = 2$) are consistent with our experimental results is $p \leq p^2 \sim 2 \times 10^{-7}$. Then, no evidence for the presence of superluminal communications is found and only a higher value of the lower bound $\beta_{t,max}$ can be established. Since the acquisitions are not synchronized with times t_{ij} , the duration time δt in eq.(5) does not coincide with the acquisition time Δt but it is $\delta t = 2\Delta t = 0.492$ s. Substituting the experimental values $\rho = 1.83 \times 10^{-7}$ and $\delta t = 0.494$ s in eq.(5) and considering the unfavorable case $\chi = \pi/2$, we get our lower bound $\beta_{t,max}$. The upper curve in Figure 6 shows our $\beta_{t,max}$ versus the unknown velocity β

of the *PF*. For *PF* velocities comparable to those of the *CMB* Frame ($\beta \approx 10^{-3}$) the corresponding lower bound is $\beta_{t,max} \approx 5 \times 10^6$. The lower curves represent the experimental values of $\beta_{t,max}$ obtained in the previous experiments [16–18]. No breakdown of quantum correlations has been observed and, thus, either the superluminal communications are not responsible for quantum correlations or their velocities are greater than $\beta_{t,max}$. Finally, it has to be noticed that remains open the possibility that $\beta_t < \beta_{t,max}$ but the *PF* velocity vector \vec{V} makes an angle $\chi < 18^\circ$ with the Earth rotation axis.

We acknowledge the Fondazione Pisa for financial support. We acknowledge the *EGO* and *VIRGO* staff that made possible the experiment and, in particular, F. Ferrini, F. Carbognani, A. Paoli and C. Fabozzi. A special thank to M. Bianucci (*Pisa Physics Department*) and to S. Cortese (*VIRGO*) for their invaluable and continuous contribution to the solution of a lot of electronic and informatic problems. Finally, we acknowledge T. Faetti for his helpful suggestions on real time procedures.

two measurements are not exactly simultaneous. When the first measurement is performed in the point *A*, a collapsing wave propagates superluminally in the space starting from *A*. The predicted *QM* correlations (e. g. the violation of the Bell inequality) occur only if the collapsing wave gets the second particle before its measurement.

- [9] N. Gisin, “Quantum correlations in newtonian space and time: Faster than light communication or nonlocality,” in *Quantum Theory: A Two-Time Success Story: Yakir Aharonov Festschrift*, edited by D. C. Struppa and J. M. Tollaksen (Springer Milan, Milano, 2014) pp. 185–203.
- [10] J. Bancal, S. Pironio, A. Acín, Y. Liang, V. Scarani, and N. Gisin, *Nat. Phys.* **8**, 867 (2012).
- [11] T. J. Barnea, J.-D. Bancal, Y.-C. Liang, and N. Gisin, *Phys. Rev. A* **88**, 022123 (2013).
- [12] B. Coccianti, *Physics Essays* **26**, 531 (2013).
- [13] B. Coccianti, *Journal of Physics: Conference Series* **626**, 012054 (2015).
- [14] A. Aspect, in *Quantum (Un)speakables: From Bell to Quantum Information*, edited by R. A. Bertlmann and A. Zeilinger (Springer, 2002).
- [15] B. Coccianti, S. Faetti, and L. Fronzoni, *Journal of Physics: Conference Series* **880**, 012036 (2017).
- [16] D. Salart, A. Baas, C. Branciard, N. Gisin, and H. Zbinden, *Nature* **454**, 861 (2008).
- [17] B. Coccianti, S. Faetti, and L. Fronzoni, *Phys. Lett. A* **375**, 379 (2011).
- [18] J. Yin, Y. Cao, H.-L. Yong, J.-G. Ren, H. Liang, S.-K. Liao, F. Zhou, C. Liu, Y.-P. Wu, G.-S. Pan, L. Li, N.-L. Liu, Q. Zhang, C.-Z. Peng, and J.-W. Pan, *Phys. Rev. Lett.* **110**, 260407 (2013).
- [19] D. Salart, A. Baas, C. Branciard, N. Gisin, and H. Zbinden, arXiv:0810.4607 [quant-ph] (2008).
- [20] P. G. Kwiat, E. Waks, A. G. White, I. Appelbaum, and P. H. Eberhard, *Phys. Rev. A* **60**, R773 (1999).
- [21] J. Altepeter, E. Jeffrey, and P. Kwiat, *Opt. Express* **13**, 8951 (2005).
- [22] G. M. Akselrod, J. B. Altepeter, E. R. Jeffrey, and P. G. Kwiat, *Opt. Express* **15**, 5260 (2007).
- [23] R. Rangarajan, M. Goggin, and P. Kwiat, *Opt. Express* **17**, 18920 (2009).
- [24] L. D. P.K. Seidelmann, B. Guinot, *Explanatory Supplement to the Astronomical Almanac, cp.2* (US Naval Observatory, University Science books, Mill Valley, CA, 1992).
- [25] International Earth Rotation and Reference Systems Service, <https://datacenter.iers.org/>.

* b.coccianti@comeg.it

† sandro.faetti@unipi.it

‡ leone.fronzoni@unipi.it

- [1] A. Einstein, B. Podolsky, and N. Rosen, *Phys. Rev.* **47**, 777 (1935).
- [2] J. S. Bell, *Physics* **1**, 195 (1964).
- [3] J. F. Clauser, M. A. Horne, A. Shimony, and R. Holt, *Phys. Rev. Lett.* **23**, 880 (1969).
- [4] J. F. Clauser and M. A. Horne, *Phys. Rev. D* **10**, 526 (1974).
- [5] A. Aspect, J. Dalibard, and G. Roger, *Phys. Rev. Lett.* **49**, 1804 (1982).
- [6] P. H. Eberhard, in *Quantum theory and pictures of reality: foundations, interpretations, and new aspects*, edited by W. Schommers (Springer-Verlag, Berlin; New York, 1989).
- [7] D. Bohm and B. J. Hiley, *The undivided universe: an ontological interpretation of quantum mechanics* (Routledge, 1991).
- [8] The key idea is that, in a typical *EPR* experiment, the